MMC and EMMC based STATCOM: A Comparative Study

K. Damodara Reddy
Assistant professor(Sr.Gd)
Vardhaman college of engg.
Hyderabad, India

N.Uma Maheshwar
Student
Vardhaman college of engg.
Hyderabad, India

K.Kalyan Kumar
Assistant professor
Vardhaman college of engg.
Hyderabad, India

ABSTRACT
This paper presents MMC based on the half-bridge converters, to achieve higher performance as a STATCOM in a distorted and unbalanced medium voltage large-current (MV-LC) system. Further, an extended MMC (EMMC) in order to manage more accurate compensation for high-power applications. Both can be controlled for various purposes such as reactive power and unbalance compensation, voltage regulation, and harmonic cancellation. Moreover, related control strategies for both the MMC and the EMMC ensure that the source-end three-phase currents are sinusoidal and balanced. Also, the dc-link capacitors of the half-bridge converters are regulated. One interesting application for the EMMC-based STATCOM could be the improvement in power quality and performance of the electrified railway traction power supply system. Both the MMC- and the EMMC-based STATCOM with Phase Shifted PWM were simulated and simulations confirm the predefined objectives**.**

Index Terms
EMMC, Harmonics, medium-voltage large-current (MVLC), MMC, unbalanced compensation

1. INTRODUCTION
Nonlinear loads such as single-phase ac traction systems make the network to operate under undesired conditions, i.e., distorted, uncontrolled reactive power and significant unbalance enforcement [1], [2]. Mitigation of all these power quality problems by means of a single compensator is a challenging task in a medium-voltage network [3], [4]. The idea of modular multilevel converters (MMC) was first introduced by Marquardt for medium-voltage applications [10]. Due to the modularity of these converters, they are very attractive for high voltage dc transmission (HVDC), flexible ac transmission systems (FACTS), and medium-voltage drives [11], [12]. The main advantage of applying the MMC as a STATCOM [13] is that they could operate under unbalanced and distorted voltages and currents properly, while voltages of the dc-link capacitors remains balanced [9]. EMMC is composed of parallel connection of multiple MMC per phase in order to deal with large-current requirements. There are two main differences between the EMMC and just parallel connection of MMC: 1) two or more MMC in an EMMC share the common dc-link (positive and negative common points); and 2), the presence of the coupling inductors that lowers down considerably the circulating current between them. The EMMC produces higher quality waveforms for the network compared to the MMC, reducing the conductive electromagnetic interference concerns in large-current applications. Also, paralleling multiple MMC improves reliability, performance, and efficiency of the overall system, making it more flexible. This paper presents the performance assessment of phase shifted PWM with PI and FYZZY controllers for MMC AND EMMC based STATCOM.

2. MMC-BASED STATCOM
The MMC-based STATCOM is composed of two parallel connected complementary HBCC as shown in Fig. 1. Each star connected HBCC has either three or four similar legs (cascaded HBM). While one HBCC has a negative common point (NCP), the other one has a positive common point (PCP). Both the NCP and PCP are float. To compensate a three-wire distorted load, the converter can be composed of two three-leg complementary HBCC. The number of levels, in a general (n + 1)-level MMC, is defined by the available n identical HBM cascaded in each leg. Then, all (n + 1)-level legs are connected to the network using an inductive filter (*LF*). All HBM have the same semiconductor ratings as well as identical dc-link capacitance. Therefore, each HBM can be assumed as an identical two-terminal device. Voltage regulation of the dc-link capacitors is achieved without any additional connections or energy transfer circuits to the associated HBM.

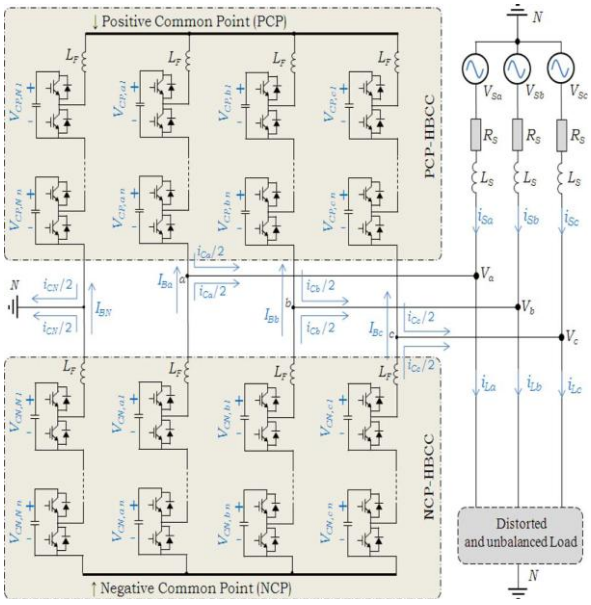

Fig. 1: Configuration of the MMC-based STATCOM.

2.1 Control Methodology

Assume that the controller unit in the MMC-based device is performing a full compensation as a STATCOM. Hence, the following tasks can be discussed.

2.2 Proper Reference Currents for STATCOM:

The general instantaneous power theory [16] was used to derive the reference currents for each output phase of the MMC-based STATCOM as described in Fig. 2(a). The objective of this compensation theory is to make the source currents completely sinusoidal and balanced; i.e., in phase with the fundamental positive sequence component of the source voltage.

When the MMC provides unbalanced currents to compensate the nonlinear unbalanced load, one output phase of the MMC may produce active power while the other phases consume active power. This causes discharge of those capacitors supplying active power, and charge of those capacitors consuming active power. Since each leg of a pair-leg supplies half of a phase current, the capacitor voltages of each pair-leg share equal changes. Meanwhile, unequal capacitor voltages of two pair legs, connected to two different phases, cause a direct balancing current (*IB*) flowing from the overcharged pair-leg toward the undercharged pair-leg [15]. Under such circumstances, the total current of each leg of the NCP-HBCC and the PCP-HBCC is equal to ($x = a, b, c, N$)

$$\begin{bmatrix} i_{Nx} \\ i_{Px} \end{bmatrix} = \begin{bmatrix} \frac{i_{Cx}}{2} + I_{Bx} \\ \frac{i_{Cx}}{2} - I_{Bx} \end{bmatrix} \quad (1)$$

Where *iNx*, *iP x*, and *iCx* are the NCP-HBCC, PCP-HBCC, STATCOM currents, respectively. The balancing current magnitude in each pair-leg (*IBx*) depends on the value of active power interchanged between the network and the pair-leg. The presence of this balancing current makes the stored energy at all legs to remain balanced. At the same time, any balancing current fluctuations are attenuated through the inductance *LF* .

2.3 Calculation of the Reference Voltage for Each Leg:

Having calculated the three-phase reference currents of the MMC- or EMMC-based STATCOM, if *VLNx* and *VLP x* are the NCP-HBCC and PCP-HBCC voltage drops on *LF* (the commutating inductance), then the three-phase reference voltages of STATCOM can be worked out as follows ($x = a, b, c$) [see Fig. 2(b)]:

$$\begin{bmatrix} V_{Nx.ref} \\ V_{Px.ref} \end{bmatrix} = \begin{bmatrix} V_x - V_{LNx} - V_{NCP} \\ V_x - V_{LPx} - V_{PCC} \end{bmatrix}$$

$$= \begin{bmatrix} V_X - L_F \dfrac{d(i_{Cx} + 2I_{Bx})}{2dt} + \dfrac{V_{DCM}}{2} \\ V_x - L_F \dfrac{(i_{Cx} - 2I_{Bx})}{2dt} - \dfrac{V_{DCM}}{2} \end{bmatrix}$$

$$= \begin{bmatrix} V_x - L_F \frac{d(i_{Cx})}{2dt} + \frac{V_{DCM}}{2} \\ V_x - L_F \frac{d(i_{Cx})}{2dt} - \frac{V_{DCM}}{2} \end{bmatrix} \quad (2)$$

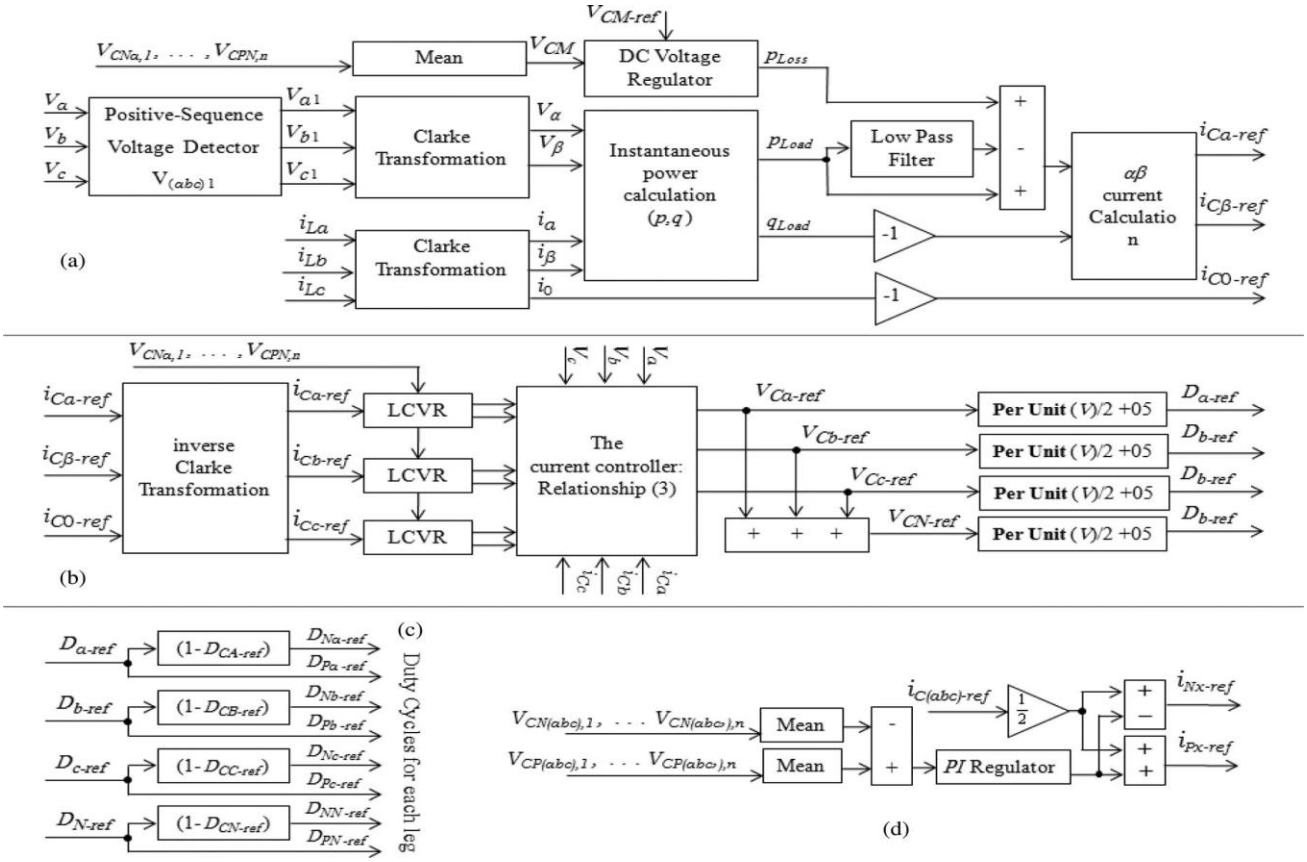

Fig. 2: Controller unit for both the MMC and the EMMC-based STATCOM, (a) derivation of the three-phase reference currents, (b) current controller diagram, (c) duty cycle extraction to generate switching modulation, and (d) local capacitor voltage regulator for both legs connected to one terminal (pair-leg).

Assume that the derivation of *IBx* is ignored in (2) for the steady-state operation of STATCOM. By neglecting the resistance associated with *LF*, (2) can be employed as a current controller for STATCOM to track the reference currents. To implement the current controller with a DSP, (2) can be represented in a discrete form with a good approximation as follows:

$$\begin{bmatrix} V_{N_{x-ref}}(Z) \\ V_{P_{x-ref}}(Z) \end{bmatrix} = \begin{bmatrix} V_x(Z-1) - \frac{L_F(i_{C_{x-ref}}(Z) - i_{C_x}(Z-1))f_{sc}}{2} + \frac{V_{DCM}}{2} \\ V_x(Z-1) - \frac{L_F(i_{C_{x-ref}}(Z))f_{sc}}{2} - \frac{V_{DCM}}{2} \end{bmatrix} \quad (3)$$

Here *x* stands for *a*, *b*, or *c*, *iCx*-ref denotes the STATCOM reference current in the phase *x*, *VNx*-ref and *VP x*-ref are the predicted reference voltage for the NCP–HBCC-leg and the NCP–HBCC-leg in the phase *x*, respectively, and *f*SC is the DSP sampling frequency of the control unit. The voltage *VCx*-ref in Fig. 2 can be obtained from (3) when both sides of (3) are normalized by *V*DCM/2 as (4) shown at the bottom of the page, where *DNx*-ref and *DP x*-ref are the duty cycles of NCP–HBCC and PCP–HBCC legs, respectively, and *VCx*-ref is the predicted reference value of the pair-leg for the phase *x*.

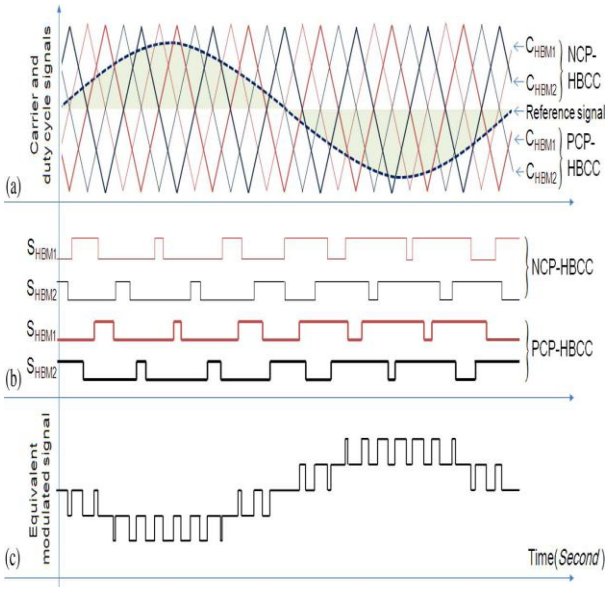

Fig. 3: Phase-shifted PWM modulation technique to create witching signals for four HBM of the MMC having two HBM per leg: (a) carrier signals of the NCP-HBCC and the 180 degrees phase shifted PCP-HBCC, (b) switching pattern generated for four HBM of the pair-leg, and (c) equivalent modulated signal.

2.4 Switching Modulation for Each HBM:

A phase-shifted PWM modulation technique is introduced in [18] and [20] for the cascaded HBM. The main goal is to share linearly the load among all HBM. Therefore, as shown in Fig.3, each HBM has an independent carrier signal, while the reference signal is shared by all the series HBM in each leg. The switching instants of each HBM are generated by the comparison of the leg reference voltage and the HBM carrier signal. To reduce the output current ripple of the MMC, the carrier signals for the NCP–HBCC are shifted by 180◦ compared to those of the PCP-HBCC correspondingly (see Fig 3). Therefore, the output current ripple of the MMC can reciprocally be canceled up to 50% in comparison with the ripples of the HBCC.

2.5 Capacitor Voltage Balancing of all HBM:

Each HBM has two complementary switches in series, providing either the dc link voltage or zero for the output. When this output voltage of the HBM is set to its dc-link voltage, a positive input current (*iNx* > 0) decreases the capacitor voltages of the NCP–HBCC, and increases those of the PCP–HBCC. Similarly, a negative input current (*iNx* < 0) increases the capacitor voltages of the NCP–HBCC, and decreases those of the PCP–HBCC. Otherwise, when the output voltage of the HBM is zero, the capacitor voltage will not change. These switching effects can be used for capacitor voltage balancing. Thus, for balanced load sharing of all HBM in a leg, the measured capacitor voltages of the leg are sorted in ascending order for each switching period. The sign of the leg current and the number of HBM that are permanently set to its dc-link voltage determine that HBM should be selected [12]. In fact, the explained algorithm is a combination of PS–PWM with a procedure that selects those HBM need to be activated among all HBM available in a leg. Instantaneous power of a pair-leg (*pNx*(*t*) and *pP x*(*t*)) can be calculated using (1) and (3), having a dc component (*PNx* and *PP x*) along with an alternative component (*pNOx*(*t*) and

$$\begin{bmatrix} V_{N_{x-ref}}(Z) \\ V_{P_{x-ref}}(Z) \end{bmatrix}_{Normalized} = \begin{bmatrix} D_{N-ref}(Z) \\ D_{p_{x-ref}}(Z) \end{bmatrix}$$

$$= \begin{bmatrix} \frac{2V_{x(Z-1)}}{V_{DCM}} - \frac{L_F(i_{C_x}-(Z)-i_{C_x}(Z-1))F_{sec}}{V_{DCM}} + 1 \\ \frac{2V_{x(Z-1)}}{V_{DCM}} - \frac{L_F(i_{C_x}-(Z)-i_{C_x}(Z-1))F_{sec}}{V_{DCM}} - 1 \end{bmatrix} = \begin{bmatrix} V_{C\,x-ref}(Z)+1 \\ V_{C\,x-ref}(Z)-1 \end{bmatrix}$$

$$= V_{C_{x-ref}}(Z) = \frac{2V_x(Z-1)}{V_{DCM}} - \frac{L_f(i_{c\,x-ref}(Z)-i_{c\,x}(Z-1))f_{sec}}{V_{DCM}} \quad (4)$$

$p_{P\,Ox}(t)$) for each leg as follows (*x* = *a*, *b*, or *c*):

$$\begin{bmatrix} PN_x(t) \\ Pp_x(t) \end{bmatrix} = \begin{bmatrix} PN_x \\ Pp_x \end{bmatrix} + \begin{bmatrix} PN_{OX}(t) \\ PP_{OX}(t) \end{bmatrix} \quad (5)$$

The dc term (nonzero average value over 50/60 Hz) is equal to

$$\begin{bmatrix} P_{Nx} \\ P_{PX} \end{bmatrix}$$

$$= \begin{bmatrix} \frac{i_{C_x}V_x}{2} - \frac{i_{C_x}L_F(i_{C_{x-ref}}-i_{C_x})f_{sec}}{4} + \frac{I_{B_x}V_{DCM}}{2} \\ \frac{i_{c_x}V_x}{2} - \frac{i_{C_x}L_F(i_{C_{x-ref}}-i_{C_x})f_{sec}}{4} + \frac{I_{B_x}V_{DCM}}{2} \end{bmatrix} \quad (6)$$

and the ac term (zero average value over 50/60 Hz) is equal to

$$\begin{bmatrix} P_{NO_x}(t) \\ P_{PO_x}(t) \end{bmatrix}$$

$$= \begin{bmatrix} I_{B_x}V_x - \frac{I_{B_x}L_F(i_{C_{x-ref}} - i_{C_x})f_{sec}}{2} + \frac{i_{C_x}V_{DCM}}{4} \\ -I_{B_x}V_x - \frac{I_{B_x}L_F(i_{C_{x-ref}} - i_{C_x})f_{sec}}{2} - \frac{i_{C_x}V_{DCM}}{4} \end{bmatrix} \quad (7)$$

Since both components in (6) are similar, the average active power is the same at 50/60 Hz for both legs of a pair-leg. Therefore, variations of the capacitor voltages for a pair-leg are the same too. Due to non ideal nature of the converter elements, there is a slight difference between the capacitor voltages of the two legs of a pair-leg. This may be corrected by using appropriate local controller to adjust current contribution for the two legs as shown in Fig. 2(d). There are four local capacitor voltage regulators in the MMC that each regulates the capacitor voltages of a pair leg. This technique assures balance of the capacitor voltages for all HBM in the converter. To regulate the dc voltage of all capacitors at a predetermined reference value, a dc voltage regulator unit is added in the reference current controller unit. The mean value of all capacitor voltages is regulated toward a certain value by estimating power losses through a dc voltage regulator unit, adding it to the reference output power of the converter as shown in Fig. 2(a).

3. EMMC-BASED STATCOM

Here the EMMC-based STATCOM is proposed for full compensation of the MV-LC loads such as electric traction systems. The suggested high power STATCOM comprises of two or more identical MMC all connected in parallel. A simple model of the EMMC-based STATCOM, having two MMC, is shown in Fig. 4. While all MMC have the same electrical specification, all NCP legs connected together, and the same is done for all PCP legs to achieve a better voltage regulation for the capacitors. Hence, voltage regulation for the HBM capacitors is managed without any additional connections or energy transfer circuits. The total output current of each phase is equally supplied by all legs coupled to that phase. For instance, each HBCC of the STATCOM, shown in Fig. 4, provides a quarter of the output current for each phase. Subsequently, for *m* parallel MMC, the nominal current rating for all HBM is specified by

$$i_{H_{max}} = \frac{\max(i_x)}{2m}\Big|_{x=a,b,c,N} \quad (8)$$

Where max (*ix*) is the maximum output current coming out of STATCOM.

The balancing current magnitude for each leg depends on the share of active power flowing into or out of that leg. It can be seen from the circuit structure (see Fig. 4) that the sum of balancing current for each HBCC is zero, namely

$$I_{Bs}+I_{Bb}+I_{Bc}+I_{BN}=0 \quad (9)$$

Therefore, considering (5) and (9), the stored energy of all legs remains balanced, a necessary condition for the capacitor voltage balancing purposes.

3.1 Switching Modulation of the EMMC:

Considering the discussed current sharing for the EMMC based STATCOM, (3) has to be rewritten in order to calculate the instantaneous reference voltages for each leg (*VNx* and *VP x*) of the EMMC-based STATCOM containing *m* parallel MMC as follows:

$$\begin{bmatrix} V_{N\,x-ref} \\ V_{P\,x-ref} \end{bmatrix} = \begin{bmatrix} V_x - \frac{L_F(i_{C_{x-ref}} - mi_{C_x})f_{sec}}{2m} + \frac{V_{DCM}}{2} \\ V_x - \frac{L_F(i_{C_{x-ref}} - mi_{C_x})f_{sec}}{2m} - \frac{V_{DCM}}{2} \end{bmatrix} \quad (10)$$

The reference voltages obtained by (10) is identical for all corresponding legs of each MMC within the EMMC. A phase-shift PWM modulation technique, similar to that of the MMC-based STATCOM, can be applied to the EMMC.

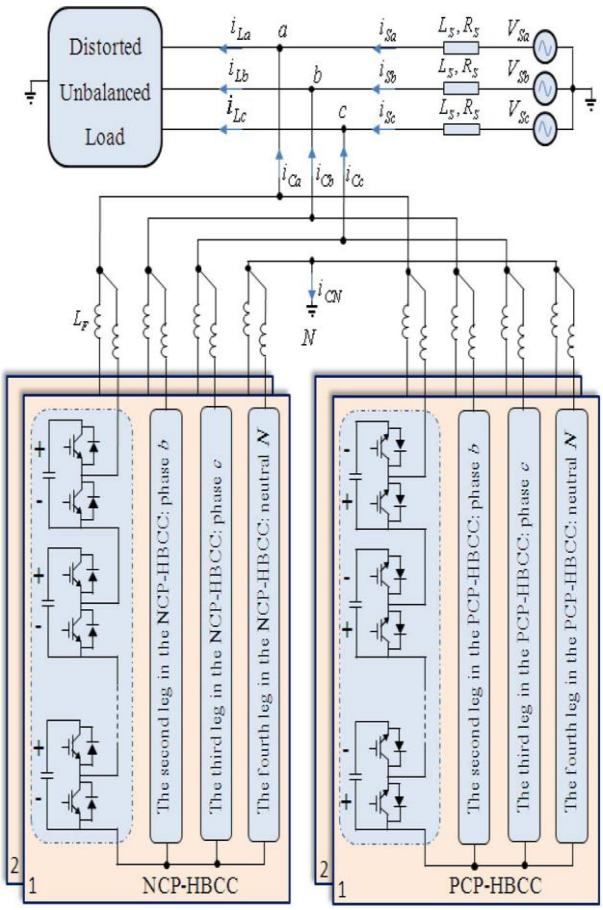

Fig. 4: Structure of the EMMC that is composed of two parallel MMC, connected to the network.

Therefore, the switching pattern for each HBM is obtained by comparing the general reference voltage with the carrier signal of each HBM as shown in Fig. 5. Carrier signals used for all shunted MMC are relatively shifted to each other to lower the output current ripple of STATCOM as follows:

$$T=\frac{1}{F_{C1}nm} \quad (11)$$

Where τ is the time interval between two adjacent carrier signals, *fC*1 is the carrier frequency, *n* is the number of HBM in each leg, and *m* is the number of MMC in the EMMC.

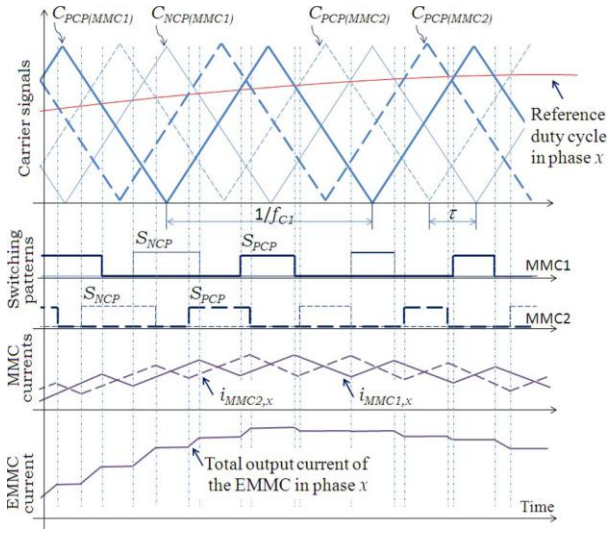

Fig.5. Illustration of the EMMC switching pattern modulation based on the phase-shift PWM, assuming the EMMC includes two MMC (their carriers are shifted by 180◦ to reduce the ripple of output current) and one HBM per leg.

3.2 Circulating Currents:

The inductance *LF* in series with each leg can substantially lower down fluctuation of the output currents. The switching signals for each HBM, in a pair-leg, are generated by different triangular carrier signals as shown in Fig. 5. Hence, because of asynchronous switching signals in those legs, the presence of a circulating current between parallel MMC (*IC*) would be unavoidable. The bigger the inductance *LF* , the lower will be this circulating current amplitude. However, increasing *LF* causes some drawbacks: decreases the controller efficiency, affects the frequency response, raises the inductor size, and increases the power losses. A solution is suggested here by inserting a coupling inductor *LC* in series with *LF* as illustrated in Fig. 6. Considering the polarity marks, *LC* shows a zero inductance in conducting common mode, being activated in differential mode. In fact, the core magnetic flux of *LC* is virtually zero when all pair-legs connected to one phase share identical currents. Hence, the total series inductance remains almost unchanged. Practically, there is an insignificant inductance due to the leakage of imperfect magnetic coupling that is negligible. Further, the small circulating current in those pair-legs is lowered by the coupling inductors effectively. It should be noted that *LC* has no effect on the balancing dc current *IB* in steady-state operation; nonetheless, this can saturate the core. Therefore, this should be considered in the filter design procedure [17].

4. SIMULATION RESULTS:

The power circuits of both MMC and EMMC-based STATCOM with PI and FUZZY controller were simulated, results are compared. Simulations were carried out using MATLAB. Assume that a 25-kV network is supplying a distorted unbalanced load in an electrical railway application. Separate simulations were arranged for both the MMC and the EMMC-based STATCOM for a power rating of ±15 MVA. Each leg of the two compensators has 22 cascaded HBM. All HBM have a dc-link capacitor with a nominal dc voltage of 3.3 kV. The minimum dc-link capacitance of each HBM is determined based on the maximum allowable ripples on top of the dc voltage as follows:

$$C_m = \frac{i_{H,max}}{f_{C1}\Delta V_{C,max}} \quad (12)$$

Where ΔVC,max is the maximum allowable voltage ripple on the dc-link voltages and $fC1$ is the basic carrier frequency.

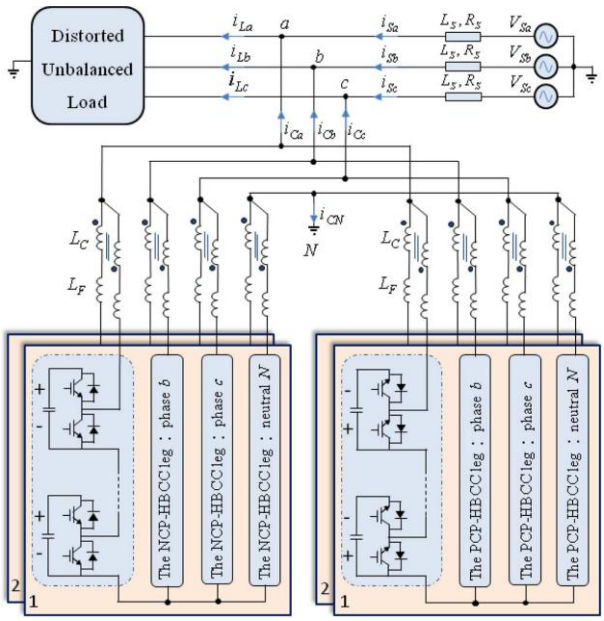

Fig. 6: Adding the coupling inductors (*LC*) in series with the filter inductors (*LF*) to reduce of the circulating current (*IC*).

Since the current controller momentarily adjusts the output current of STATCOM, variation of the dc-link voltages in the allowable region will not disrupt the compensator operation. For the EMMC-based STATCOM, having two MMC, *LF* and *LC* contribute to the attenuation of a sudden rise of the balancing current *IBx* and the circulating current *IC* due to an abrupt change in the load currents. Since the total series inductance *LS* is almost identical for both the EMMC and the MMC, *LS* is calculated according to the maximum allowable ripple on the output currents ΔiC,max as below

$$L_S = L_F + L_C = \frac{V_{DCM}}{mn}\frac{T_S}{\Delta i_{C,max}} = \frac{V_{DCM}}{mnf_{c1}\Delta i_{C,max}} \quad (13)$$

Here, the PS–PWM modulation technique is applied to both compensators with a switching frequency of $fC1$ = 1000 Hz.. Simulations are shown in Fig. 7, where Fig. 7(a)–(f) illustrates the PCC voltages, load currents, the EMMC currents, the source-end currents after compensation with the EMMC-based STATCOM, the MMC currents and the source-end currents after compensation with the MMC-based STATCOM, respectively. It can be seen from Fig. 7(d) and (f) that while both MMC and EMMC balance the source-end currents, the EMMC-based STATCOM produce much smoother currents than those of the MMC. Additionally, the source-end currents are in phase with the fundamentals of positive sequence voltages, containing no reactive components. Since each leg has 22 HBM, the equivalent

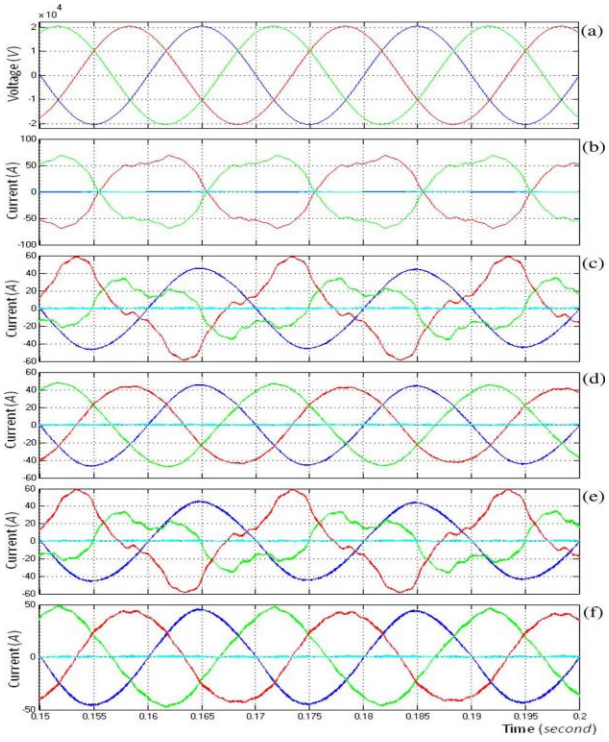

Fig. 7: Voltage and current waveforms: (a) voltages of the PCC, (b) load currents, (c) EMMC currents, (d) source-end currents after compensation by the EMMC-based STATCOM, (e) MMC currents, and (f) source-end currents after compensation by the MMC-based STATCOM

EMMC1fuzzy

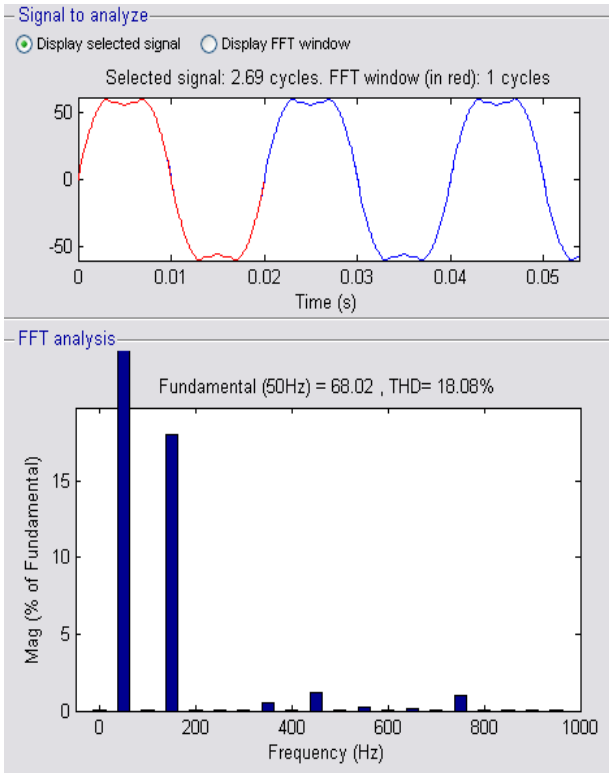

Fig. 8: Load current THD

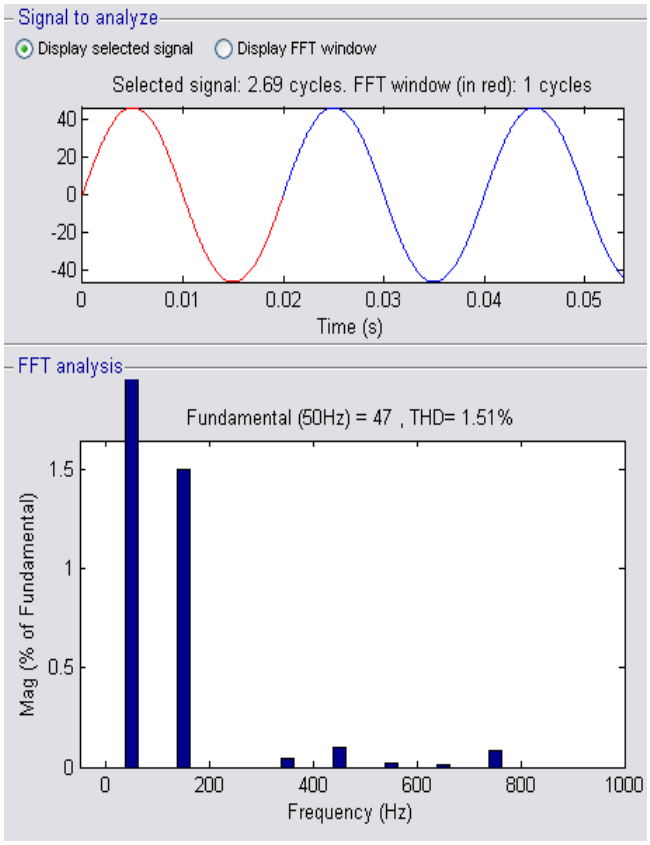

Fig. 9: Source current THD MMC1fuzzy

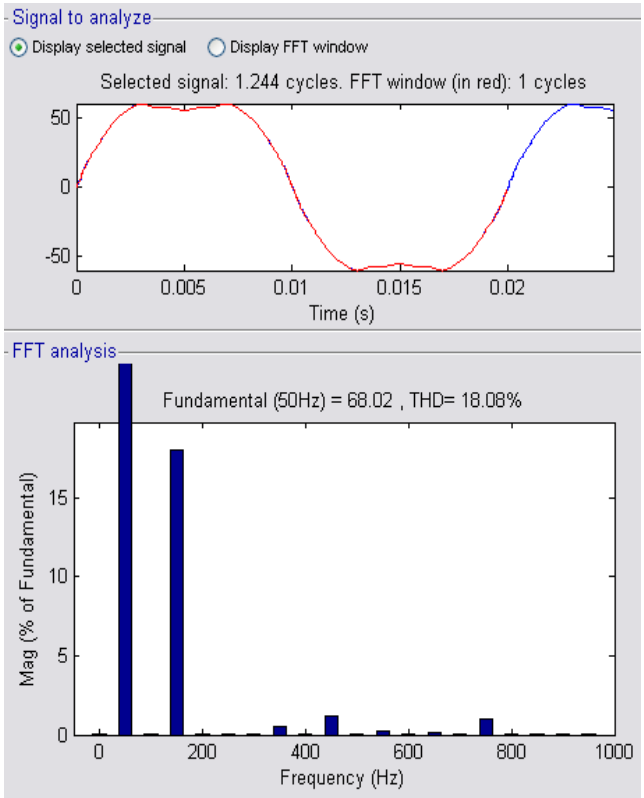

Fig. 10: Load current THD

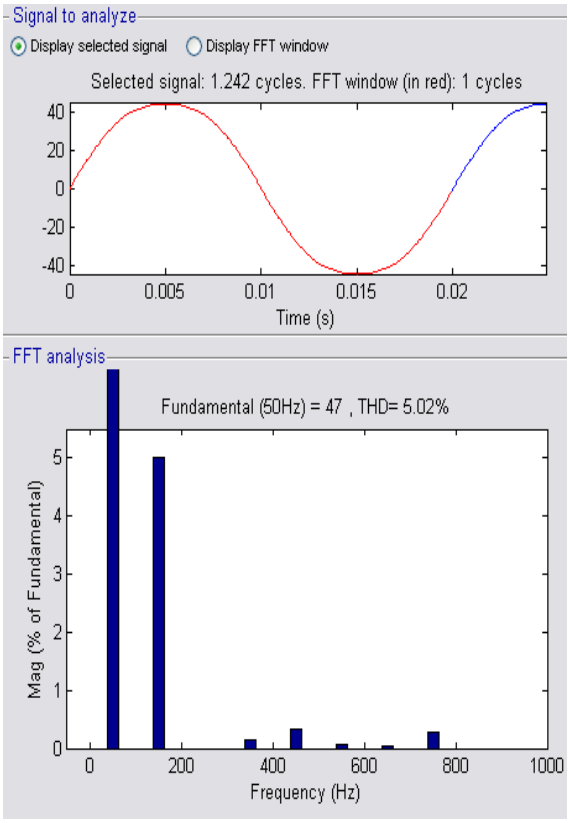

Fig. 11: Source current THD

Considering the performed simulations and experiments, although the MMC-based STATCOM is capable of full compensation, the EMMC-based STATCOM presents the following additional advantages:
1) Providing smoother output currents, smaller power losses, and improving the harmonic performance.
2) Generating higher reactive power rating with lower dc-link voltages; this implies lower voltage rating for the dc capacitor and lower stress on the switches.
3) Operating with a smaller switching frequency, resulting in smaller switching losses.
4) Increasing the reliability of the compensator even if one MMC is out of order.
Therefore, the EMMC presents higher energy efficiency, lower heat dissipation, lower weight and volume for the compensator. In fact, the EMMC has lower maintenance costs compared to the MMC. In the mean time, the high-power load compensation in the MV-LC networks using the MMC-based STATCOM is usually limited by the available semiconductor technology due to the voltage and current ratings, losses and switching frequency.

5. CONCLUSION

This paper presents the performance assessment of phase shifted PWM with PI and FYZZY controllers for MMC AND EMMC based STATCOM. This modular MMC based STATCOM introduces a transformer less design, employing several isolated units composed of a number of cascaded HBM. Then, the EMMC-based STATCOM has higher efficiency, higher reliability, lower weight and size, lower switching frequency and lower ratings for the switches.

ACKNOWLEDGMENTS

The authors would like to thank the all electrical staff members of Vardhaman College of engineering.

REFERENCES

[1] P.-C. Tan, R. E. Morrison, and D. G. Holmes, “Voltage form factor control and reactive power compensation in a 25-kV electrified railway system using a shunt active filter based on voltage detection,” *IEEE Trans. Ind. Appl.*, vol. 39, no. 2, pp. 575–581, Mar./Apr. 2003.

[2] M. T. Bina and M. D. Panahlou, “Design and installation of a 250 kVAr D-STATCOM for a distribution substation,” *Elsevier: Electric Pow. Syst. Res.*, vol. 73, no. 3, pp. 383–391, Apr. 2005.

[3] F. Z. Peng and J. Wang, “A universal STATCOM with delta-connected cascade multilevel inverter,” in *Proc. 35th Annu. IEEE Pow. Electron Spec. Conf.*, Aachen, Gennany, Jun. 2004, pp. 3529–3533.

[4] R. E. Betz, T. Summerst, and T. Furney, “Using a cascaded H-bridge STATCOM for rebalancing unbalanced voltages,” in *Proc. 7th Int. Conf. Pow. Electron.*, Daegu, Korea, Oct. 2007, pp. 1219–1224.

[5] F. Z. Peng, J. Wang, McKeever, and D. J. Adams, “A power line conditioner using cascade multilevel inverters for distribution systems,” *IEEE Trans. Ind. Appl.*, vol. 34, no. 6, pp. 1293–1298, Nov./Dec. 1998.

[6] H. Akagi, S. Inoue, and T. Yoshii, “Control and performance of a transformerless cascade PWM STATCOM with star configuration,” *IEEE Trans. Ind. Electron.*, vol. 43, no. 4, pp. 1041–1049, Jul./Aug. 2007.

[7] C. K. Lee, J. S K. Leung, S. Y R. Hui, and H. S. H. Chung, “Circuit-level comparison of STATCOM chnologies,” *IEEE Trans. Pow. Electron.*, vol. 18, no. 4, pp. 1084–1092, Jul. 2003.

[8] R. E. Betz, T. Summers, and T. Furney, “Symmetry compensation using an H-bridge multilevel STATCOM with zero sequence injection,” in *Proc. Ind. Appl. Conf.*, Oct. 2006, pp. 1724–1731.

[9] H. M. Pirouz and M. T. Bina, “New transformerless STATCOM topologyfor compensating unbalanced medium-voltage loads,” in *Proc. 13th Eur. Conf. Pow. Electron. Appl.*, Barcelona, Spain, Sep. 2009, pp. 1–9.

[10] R. Marquardt, “Stromrichters chaltungenmitverteilten Energiespeichern,” German Patent DE 10 103 031, Jan. 24, 2001.

[11] S. Rohner, S. Bernet, M. Hiller, and R. Sommer, “Modulation, losses and semiconductor requirements of modular multilevel converters,” *IEEE Trans. Ind. Electron.*, vol. 57, no. 99, pp. 2633–2642, Aug. 2009.

[12] J. Rodr´ıguez, S. Bernet, B. Wu, J. O. Pontt, and S. Kouro, “Multilevel voltage-source-converter topologies for industrial medium-voltage drives,” *IEEE Trans. Ind. Electron.*, vol. 54, no. 6, pp. 2930–2945, Dec 2007.

[13] C. D. Schauder, “Advanced static var compensator control system,” U.S. Patent 5 329 221, Jul. 12, 1994.

[14] M. T. Bina and A. K. S. Bhat, “Averaging technique for the modeling of STATCOM and active filters,” *IEEE*

Trans. Pow. Electron., vol. 23, no. 2, pp. 723–734, Mar. 2008.

[15] M. Hagiwara and H. Akagi, "Control and experiment of pulse-widthmodulated modular multilevel converters," *IEEE Trans. Pow. Electron.*, vol. 24, no. 7, pp. 1737–1746, Jul. 2009.

[16] H. Akagi, E. Watanabe, and M. Aredes, *Instantaneous Power Theory and Applications to Power Conditioning*. Hoboken, NJ: Wiley, 2007.

[17] L. Asiminoaei, E. Aeloiza, P. N. Enjeti, and F. Blaabjerg, "Shunt activepower- filter topology based on parallel interleaved inverters," *IEEE Trans. Ind. Electron.*, vol. 55, no. 3, pp. 1175–1189, Mar. 2008.

[18] J. Rodr´ıguez, J. Lai, and F. Z. Peng, "Multilevel inverters: A survey of topologies, controls, and applications," *IEEE Trans. Ind. Electron.*, vol. 49, no. 4, pp. 724–738, Aug. 2002.

[19] Q. Song and W. Liu, "Control of a cascade STATCOM with star configuration under unbalanced conditions," *IEEE Trans. Pow. Electron.*, vol. 24, no. 1, pp. 45–58, Jan. 2009.

[20] R. Naderi and A. Rahmati, "Phase-shifted carrier PWM technique for general cascaded inverters," *IEEE Trans. Pow. Electron.*, vol. 23, no. 3, pp. 1257–1269, May 2008.